Applied Surface Science 436 (2018) 720–731

Contents lists available at ScienceDirect

Applied Surface Science

journal homepage: www.elsevier.com/locate/apsusc

Full Length Article

X-ray photoelectron spectroscopy on 1-peso and 2-pesos of the Argentine Republic

Faramarz S. Gard[a,*], Gustavo Duffo[a,b,c], Pablo Bergamasco[a], Elena Forlerer[a]

[a] Comisión Nacional de Energía Atómica, Gerencia Materiales, Argentina
[b] Universidad Nacional de San Martín, Argentina
[c] Consejo Nacional de Investigaciones Científicas Y Técnicas (CONICET), Av. Gral. Paz 1499, (1650) San Martín, Buenos Aires, Argentina

ARTICLE INFO

Article history:
Received 11 October 2017
Received in revised form 1 December 2017
Accepted 6 December 2017
Available online 9 December 2017

Keywords:
XPS
Surface segregation
Cu(I) oxide
Cu(II) oxide
Ni oxide

ABSTRACT

Relative concentrations of nickel and copper at the surface of the ring and centre parts of 1-peso and 2-pesos Argentine coins have been studied by means of X-ray photoemission spectroscopy (XPS). It has been observed Ni-enrichment at the surface of the ring (silvery) part of a 1-peso, minted in 1994, whereas the XPS data reveals lack of nickel at the surface of the centre (silvery) part of a 2-pesos, minted in 2016. This discrepancy is explained by analyzing the XPS peaks of oxygen and carbon, and is suggested to be related to the contamination layer on the surface of the coins. The XPS analysis of the golden parts of the coins, namely the centre part of the 1-peso and the ring part of the 2-pesos coins were inconclusive, due to the small amount of the Ni (nominally %2) used in those parts. The possible oxidations states of the metals at the surface of the untreated and treated coins with the artificial human sweat were also identified.

1. Introduction

Due to the physicochemical properties of the nickel, and its silvery bright finish, this metal is used in different daily objects, such as jewelry, buttons, belt buckles, and door handles and so on. It has also been used heavily to mint coins all over the world, since it has some advantages in comparison to the other silvery metals, such as price, color, density, and the ease of minting. However, the community of contact dermatologists has been alarmed that eczema related to Ni allergy has been on rise due to usage of these coins. It has been estimated that around 10-30% of women and 1-3% of men suffer of Nickel allergy [1]. The difference between the prevalence of nickel allergy in men and women is explained by the fact that the women are using more objects containing nickel than the men do [2]. The American Contact Dermatitis Society, in 2008 named the nickel as the Ällergen of the Yeardüe to abundant cases of contact allergy with nickel [3].

The problem with the nickel release from the Ni-containing coins is not new. To our knowledge nickel release from silver/nickel alloy of Swedish coins were reported for the first time in 1974 [4]. In this reference, the authors reported not only the Ni release from the coins that contain nickel, but also inform the Ni contamination on the other coins (not containing Ni) and even on the bank notes. Nevertheless, a serious debate over the Ni release of the coins and its health hazardous was triggered after circulation of euro coins in all twelve EU countries, in January 2002, and by publication of a brief communication in the journal Nature [5] in September 2002. The authors, in this reference, report a release of 240 to 320 times more nickel than it is allowed under the European Union Nickel Directive [6]. This phenomenon is explained by the fact that the coins central part and the ring part contain different amounts of nickel, copper and zinc, (see Table 1). This fact encourages galvanic corrosion process during prolonged exposure to human sweat. This was confirmed by submerging a one Euro coin and a Swiss one-franc coin, which contains 25% nickel and 75% copper, in artificial human sweat for 36 hrs: The 1- euro coin was visibly corroded, whereas a Swiss 1-franc coin was not.

Medical aspects of the Ni release from the coins, containing Ni, from different currencies have been heavily studied [8], and the references therein. However to our knowledge, there has been only one study which XPS as the main technique was used to investigate the metallic composition on the surface of the Euro coins [9]. The authors, in this reference, present XPS studies of the central and the ring part of two Dutch 1-euro coins. The results from the untreated coins, directly off the normal circulation, are compared with the polished and oxidized bulk alloy surfaces. They report significant nickel enrichment on the surface of both the ring and the centre parts of the untreated coins. The coins used in that study was

* Correponding author.
E-mail address: fsgard01@gmail.com (F.S. Gard).

https://doi.org/10.1016/j.apsusc.2017.12.052
0169-4332/

Table 1
Metallic concentrations of euro coins [7].

Coin	Composition
1 euro-ring (golden) part	1-layer: Cu 75, Zn 20, Ni 5
1 euro-central (silvery) part	3-layers: Cu 75, Ni 25//Ni 100//Cu 75, Ni 25
1 euro-ring (golden) part	1-layer: Cu 75, Zn 20, Ni 5
1 euro-central (silvery) part	3-layers: Cu 75, Ni 25//Ni 100//Cu 75, Ni 25

Table 2
Atomic concentration of Ni, Cu and Zn metals measured by XPS on the ring and centre part of two Dutch 1-euro coins (A and B), reference [9].

	Ring			centre	
	Ni	Cu	Zn	Ni	Cu
Bulk (official composition)	5.4	75.1	19.5	26.5	73.5
Untreated surface (A)	9	58	33	55	45
Untreated surface (B)	10	65	25	42	58

minted in 1999. The paper was published in 2004, so we estimate that the coins had been in circulation for almost to 5 years. Table 2 below summarizes their results from reference [9].

Nevertheless, we believe that a much more detailed XPS studies of the Ni-containing coins is needed in order to present a comprehensive view of the Ni segregation from the alloy used to mint the coins. In the present work, we have used XPS to study Argentine 1- and 2- pesos coins. The main components of these coins, similar to euro coins, are copper and nickel, with an exception that in the Argentine coins, zinc is replaced by aluminum in comparison to the euro coins, see Table 3. High resolution XPS spectra were collected from the untreated coins and treated coins with the artificial sweat. The possible corrosion products of the alloys were identified.

The official atomic concentration of the metals used to mint Argentine coins as published by the Central Bank of Argentina (CBA) are listed in Table 3. Nevertheless, we have also measured the actual composition of a 1-peso coin using Arc-Spark Optical Emission Spectroscopy (Arc-Spark OEM) technique. We followed the standard operation procedure of ASTM E415-99a: Standard Test Method for Optical Emission Vacuum Spectrometric Analysis of Carbon and Low-Alloy Metals. The uncertainty in our measurement was estimated to be 0.1%. The results are also given below in Table 3. There are some small discrepancies between the official information and our measurements. We have no knowledge of the process and the accuracy of preparing the alloys to mint the coins, and our inquiries from the (CBA) are unanswered. Therefore, we cannot comment on these discrepancies, except that, similar to Argentine coins, the values of the official composition of the euro coins reported in ref. [9] are also different than those, published by the European Central Bank (ECB), see Table 1 in comparison to the Table 2.

2. Experimental method

A 1-peso coin from 1994 and a 2-pesos coin from 2016, without any *ex situ* cleaning or pretreatment with the artificial human sweat, along with the standard samples of pure copper and nickel were introduced to the XPS chamber. XPS analysis was carried out in a PHI 5000 VersaProbeII. The base pressure in the chamber was in the range of 10^{-7} - 10^{-8} Pa. A monochromatic aluminum Kα X-ray source (100μ, 25W, 15 kV) was used to probe the samples. An Argon-etched, polished fine grained silver sample was used earlier to measure resolution of the system. The Full Width at Half Maximum (FWHM) of the $3d_{5/2}$ peak of the silver sample was measured to be 0.49 eV. All the Survey scans were collected under the following conditions; Energy Range: 0-1100 eV, the Pass Energy (PE): 187.85 eV, the step size: 0.8 eV, and the time per step was 50 ms. For the high resolution scans the PE was set to be 23.5 eV and the step size changed to 0.1 eV. Spectra were analyzed using CasaXPS software version 2.3.18.

3. Experimental results

In order to eliminate any ambiguities in the identification of the metals (Ni, Cu) and their relevant states of oxidations on the surface of the coins, XPS spectra under the same experimental conditions were collected from Cu- and Ni-standard samples. The XPS spectra collected from the standard samples are particularly essential to analise XPS spectra from the metallic alloys of copper and nickel used to mint the coins. The $2p_{3/2}$ XPS peak of the $Cu^{(0)}$, $Cu^{(I)}$ oxide, $Cu^{(II)}$ oxide, and $Cu^{(II)}$ hydroxide are reported in a narrow range of binding energy of (932.6 -934.6) eV [10]. The 2p region of the XPS spectra of Ni and Ni oxides is rich in features. This can make the chemical quantification of Ni and its oxides, based on the position of the XPS peak, more demanding. The spectra consist of asymmetric peaks, shake-up satellites, and high intrinsic background. The peak fitting process of the samples containing Ni is potentially complex due to multiplet splitting of the Ni $2p_{3/2}$ XPS peak of $Ni^{(0)}$, $Ni^{(I)}$ oxide, and $Ni^{(II)}$ oxide [11].

The standard samples were etched for 10 min by 2 KeV Ar^+ ions, in order to remove the native oxide or hydroxide and carbon from the surface. The raster size was set to be 2×2 mm. The Ni $2p_{3/2}$ XPS spectrum collected from a Ni 99.98% sheet of 0.5 mm, provided by Sigma-Aldridge, is shown in Fig. 1. Two satellite peaks and their binding energy above the main peak of $Ni^{(0)}$ at (852.5 ± 0.1) eV are indicated in the graph. The position of the binding energy of the main line and the additional satellites above the main emission line are in good agreement with the reported values in reference [11], within the uncertainty of our measurements. These satellite structures are suggested to be associated to the energy losses corresponding to the surface and bulk plasmons [11], in contrast to the previous study, where it is suggested that they are related to the holes in the final state of $c3d^94s^2$ (c is a core hole) [12].

Fig. 2 shows the photoemission spectrum of Cu $2p_{3/2}$ collected from a Cu 99.98% foil of 0.5 mm, provided by Sigma-Aldridge, in the range of 928-938 eV. A single Gaussian (70%)-Lorentzian (30%) peak defined as GL(30) in CasaXPS is fitted at binding energy of (932.59 ± 0.05) eV with a FWHM of 1.3 eV. This was expected, as we routinely calibrate the energy analyzer based on the values of the binding energies for Cu $2p_{3/2}$ and Au $2p_{3/2}$ peaks, namely 932.62 eV and 83.96 eV, respectively, as recommended by ISO standard procedure.

Table 3
Official metallic concentration (in % weight) of Argentine coins published by the CBA, and measured by Arc-Spark OEM.

Coins	Color	Composition
$1-peso[a]	Silvery (ext. part) / Golden (central part)	Cu 75, Ni 25 / Cu 92, Al 6, Ni 2
$2-pesos[a]	Golden (ext. part) / Silvery (central part)	Cu 92, Al 6, Ni 2 / Cu 75, Ni 25
$1-peso[b]	Silvery (ext. part) / Golden (central part)	Cu 76.1, Ni 23.9 / Cu 90.9, Al 7.5, Ni 1.6

[a] According to the official information the Central Bank of Argentina (CBA).
[b] Measured by Arc-Spark OEM, the uncertainty estimated to be 0.1%.

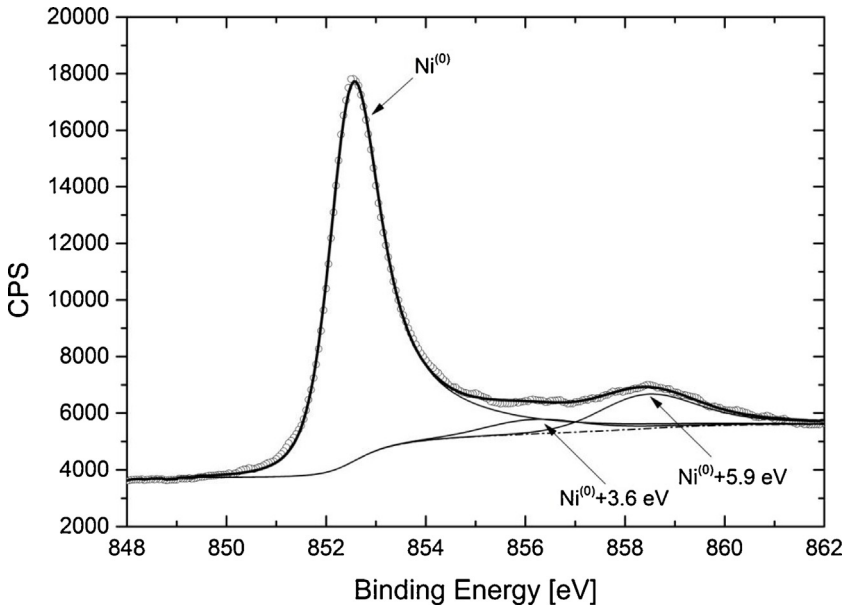

Fig. 1. Ni $2p_{3/2}$ spectrum from the nickel standard sample.

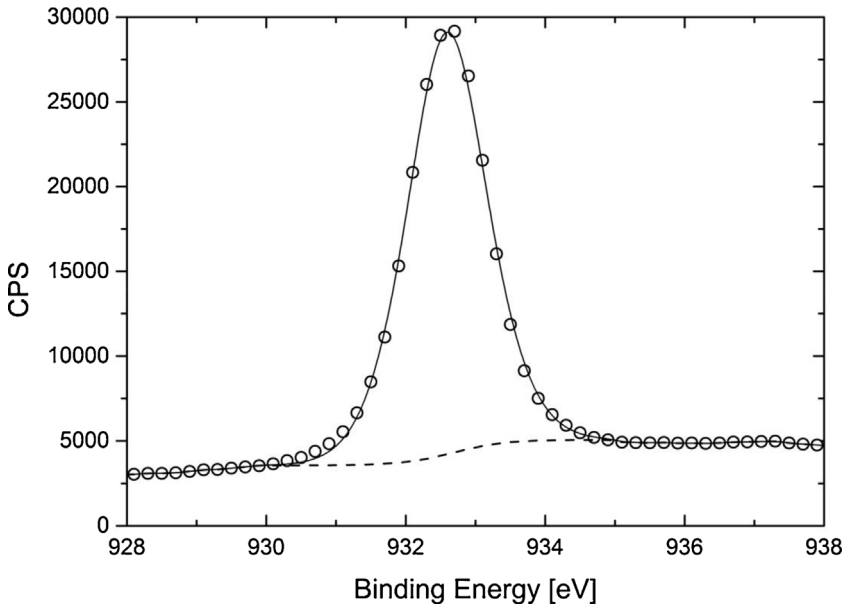

Fig. 2. Cu $2p_{3/2}$ spectrum from the copper standard sample.

3.1. XPS spectra of the untreated coins

The coins were etched for 1 min with high energy of Ar^+ of 2 keV in order to sputter the most top layer of the contamination (oxygen and carbon in form of organic and inorganic) off the surface. A moderate erosion time has been chosen to minimize the erosion of the metals and metal oxides of the coin. The raster size was set to (2×2 mm). The energy of the Ar^+ ions was then reduced to 1 keV and a depth profile was acquired with the steps of 2-minute interval. A lower energy of the Ar^+ ions was chosen in order to achieve a moderate erosion rate. It is also important to reduce the reduction effect of metal oxide due to Ar^+ ion bombardment. The erosion rate of the Ar^+ ions was pre-calibrated using a Si standard sample with a 100 nm thick SiO_2 overgrown layer. The erosion rate of Ar^+ ions with an energy of 1 keV and raster size of (2×2 mm) was estimate to be (1.0 ± 0.2) nm/min. A typical Cu 2p spectrum is shown in Fig. 3. It is collected from the ring part of the 1-peso coin of 1994 after 5 cycles of (2 min) of 1 keV Ar^+ ions sputtering. The main transition line is fitted with a major peak at (932.60 ± 0.05) eV corresponding to $Cu^{(0)}$ and a smaller peak at (933.8 ± 0.1) eV, which is assigned to be due to existence of $Cu^{(II)}$ oxide on the surface. A Shirley background type was applied to remove the contribution of the inelastic electron scattering. We have employed GL(30) peak shape to fit both components of Cu $2p_{3/2}$. Two additional small structures (Shake-up satellites) are observed in the range 940-947 eV in the Cu 2p spectrum. Many authors use these structure as an evidence of existence of $Cu^{(II)}$ rather than $Cu^{(I)}$ [13,14,15].

Table 7 in Ref. [16] lists the binding energies of $Cu^{(0)}$, $Cu^{(I)}$, $Cu^{(II)}$ compiled from a survey of the references in the NIST database [10]. The authors also present their own results from a series of standard samples in Table 8 in Ref. [16]. We have summarized those values in the Table 4. Remarkably, the authors achieved a statistical sepa-

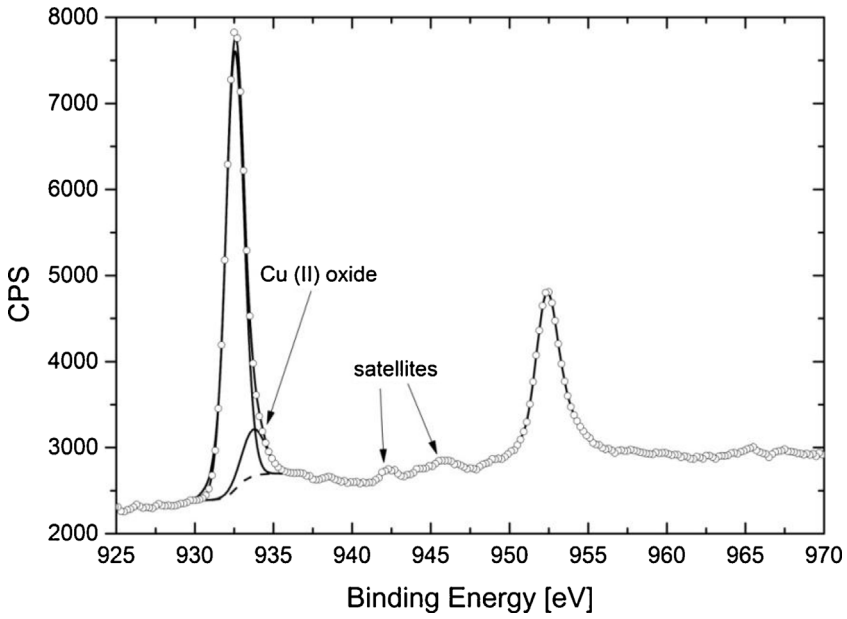

Fig. 3. Cu 2p XPS spectrum of the 1-peso coin of 1994.

Table 4
Peak positions of Cu $2p_{3/2}$ binding energy compiled from reference 10, and 16.

Compound	Cu $2p_{3/2}$ [eV][a]	Cu $2p_{3/2}$ [eV][b]
$Cu^{(0)}$	932.61	932.63
$Cu^{(I)}$	932.43	932.18
$Cu^{(II)}$ oxide	933.57	933.76
$Cu^{(II)}$ hydroxide	934.75	934.67

[a] From reference [10].
[b] From reference [16].

Table 5
Ni $2p_{3/2}$ values for Nickel from current study and compiled from reference [18].

Compound	Peak 1	Peak 2	Peak3	Peak4
[a]$Ni^{(0)}$	852.6	856.3	858.7	N/A
[a]$Ni^{(II)}$	853.7	855.4	860.9	864.0
[b]$Ni^{(0)}$	852.5	856.3	858.7	N/A
[b]$Ni^{(II)}$	853.7	855.0	861.2	Not detected

[a] From [18].
[b] Current study.

ration of the peak positions for $Cu^{(0)}$ and $Cu^{(I)}$, in comparison to the reported values in ref. [10]. It can be seen that, within the uncertainty in our measurement, the positions of the Cu $2p_{3/2}$ of $Cu^{(0)}$ and $Cu^{(II)}$ peaks of the untreated 1-peso are in a good agreement with the reported values in [16].

Identification and quantification of the nickel oxide and nickel hydroxide, like other transition metals, based on the XPS spectra comes with a large uncertainty. The Ni 2p transition lines of the oxide and hydroxide are relatively complex, they can contain multiplet splitting of the main line and the contributions of the satellite structures [11]. Therefore, many authors are using a simple peak identification technique based on a three-peaks model namely $Ni^{(0)}$, $Ni^{(I)}$, and $Ni^{(II)}$ to interpret the Ni $2p_{3/2}$ XPS spectra [17]. In the current study, we interpret and fit the Ni 2p spectra based on the studies done by M. C. Biesinger et. al. [18]. The authors compiled a comprehensive list of possible peaks associated to Ni metal and Ni oxide and hydroxide, Table 1 in Ref. [18].

Fig. 4 shows the spectrum of Ni $2p_{3/2}$ collected from the ring part of the 1-peso of 1994 after 5 cycles of (2 min) of 1 keV Ar^+ ions sputtering. A Shirley background type was applied to remove the contribution of the inelastic electron scattering. The spectrum is fitted with an asymmetric line shape both for Ni and Ni oxide and its respective plasmon loss peaks. The parameters of the components of the Ni metal peak and its plasmon loss peaks are compelled from the standard sample presented above. An empirical fitting process was applied using all the possible options suggested in reference [18] for Ni oxide and Ni hydroxide. The absolute values of binding energy were constrained within a range of ± 0.3 eV of the suggested values in the reference [18], and the best possible fitting was achieved using the multiplet splitting of $Ni^{(0)}$ and $Ni^{(II)}$, namely NiO line and its respective satellite lines. The analysis of the O 1s transition line, which is presented below also confirms the existence of the Ni oxide in a chemical state of $Ni^{(II)}$.

The main transition line is fitted with a major peak at (852.5 ± 0.1) eV corresponding to $Ni^{(0)}$. The corresponding binding energy values of the plasmon loss peaks of $Ni^{(0)}$, along with the those of the $Ni^{(II)}$ are listed in the Table 5. The respective binding energies of $Ni^{(0)}$ and $Ni^{(II)}$ taken from reference [18] are also presented. In the current study, the plasmon loss peak of the $Ni^{(II)}$ at binding energy of 864.0 eV was not detected. It is expected, as the amount of NiO on the surface of the coins is small in comparison of the pure NiO standard sample used in reference [18].

Depth profiling was performed on three different locations on the surface of the silvery part of the 1-peso and 2-pesos coins, in order to achieve a better statistical evaluation of the ratio of Cu to Ni. Fig. 5 shows part of the depth profiling (15 nm) of the 1- and 2- pesos coins. The evolution of the relative atomic concentration of Cu and Ni for the ring (silvery) part of the 1-peso of 1994 and the centre (silvery) part of the 2-pesos of 2016 are compared in the diagram.

It has been estimated that the relative concentration of Cu/Ni at the surface just after removing the first layer of the contamination, with 2 keV Ar^+ ions for one minute, is about (67%/33%) for the 1-peso coin of 1994, whereas for the coin of 2-pesos of 2016 is about (93%/7%). The concentration of Ni reaches a maximum value of ~36% for the 1-peso coin at the depth of 4-5 nm. The values which are plotted in the Fig. 8 are the average values of the results obtained from three different locations on the coins. The relative concentration ratio is getting close to the official data of 75%/25% in the range of 10 to 15 nm depth. In our calculation of the metal concentrations,

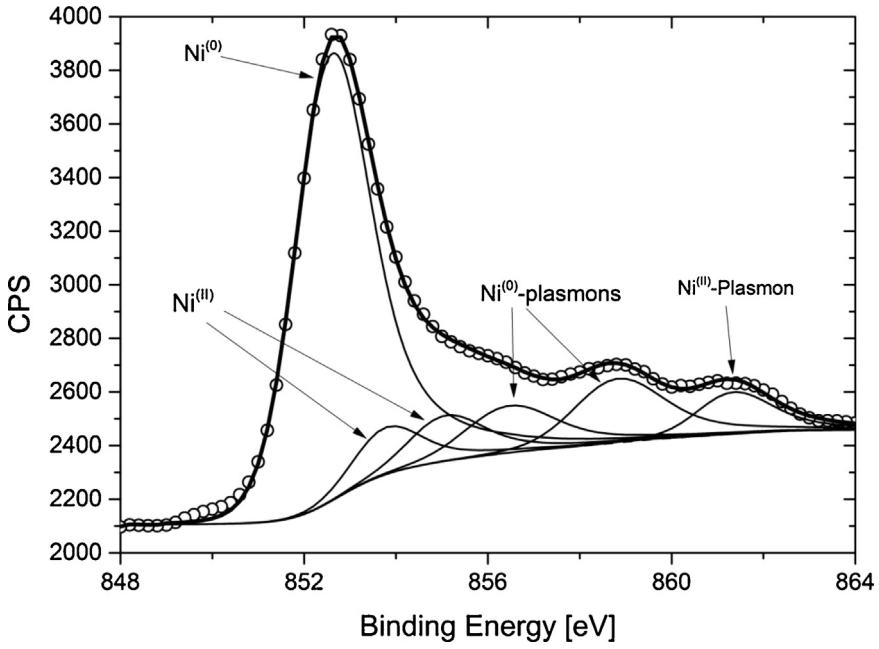

Fig. 4. Ni 2p spectrum from the silvery part of the 1-peso coin of 1994.

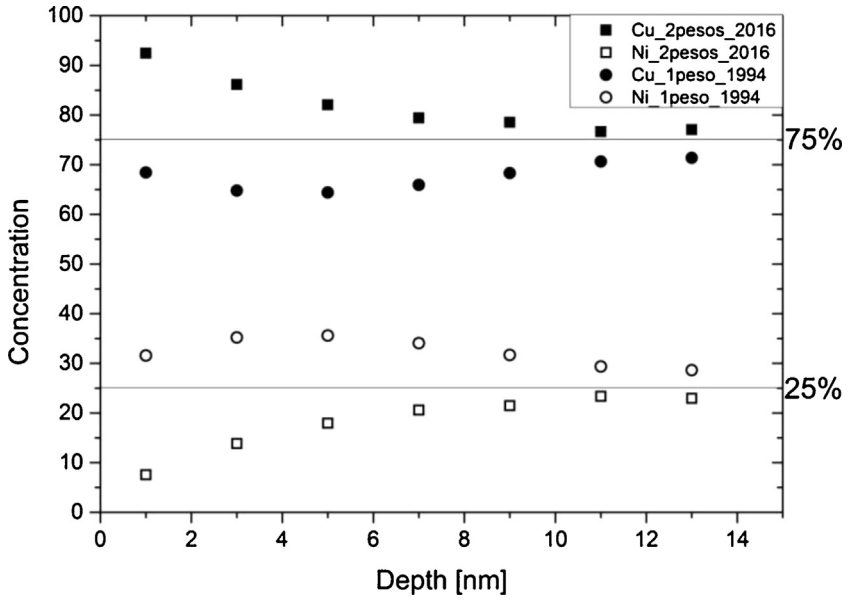

Fig. 5. Depth profiling (15 nm) of the silvery part of the 1- and 2-pesos coins.

we have included the contribution of the Ni oxide, and Cu oxide but excluded the Ni satellite and Ni oxide satellite peaks.

A Ni-enrichment was observed at the surface of the 1-peso coin, which has been in circulation more than 20 years, whereas we detected a lack of nickel at the surface of the 2-pesos coin of 2016. We have not been able to monitor similar Ni enrichment on the centre (golden) part of the 1-peso coin and the ring (golden) part the 2-pesos coin. It was expected as the nominal value of the Ni concentration on the golden part of the coins is 2% of the total.

Fig. 5 reveals that, at least to a depth of ~ 10 nm, the amount of Ni, for the 2-pesos coin, is much less than that of the official data, whereas for the 1-peso coin is the reverse. This discrepancy between the Ni/Cu atomic ratio for the new and the old coins can be explained by considering the layer of contamination containing mainly carbon (C) and oxygen (O) (in different forms of organic and non-organic), which has accumulated on the surface of the coins during the circulation time. We have discussed this in details below in the Discussion section.

The high resolution spectra of the C 1s and O 1s peaks of the new and the old coins show totally different characteristics. We estimated that the thickness of the contamination layer on the old coin is significantly greater than that of the new coin. Visual inspection of the coins also confirmed our finding. The 1-peso coin lost its shine and it looked more dull than the new 2-pesos coin of 2016.

Fig. 6(A, B) shows the C 1s transition lines of the adventitious carbon (AdC) collected from the silvery part of the 2-pesos of 2016 and the 1-peso of 1994 coins, respectively. They are collected after sputtering the sample with the 2 keV Ar^+ ions for a period of 1 min.

A quantitative comparison of the XPS transition lines from two different samples is not a good practice, and we are not attempting

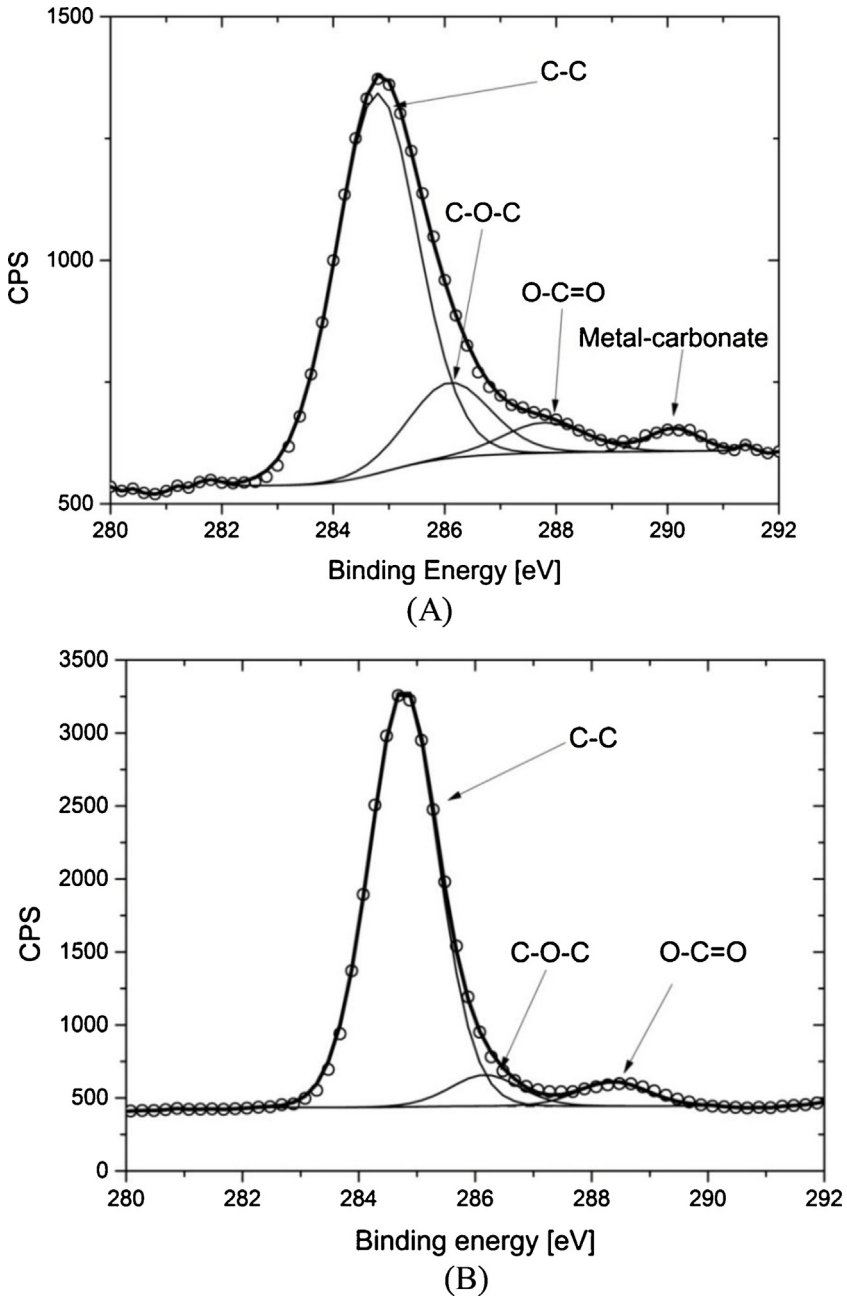

Fig. 6. C 1s spectra from silvery part of the 1-peso coin of 1994 (A) and the 2-peso coin of 2016 (B).

to do that. However, by a rough assessment of the C 1s peaks, we can estimate that the AdC on the surface of the 1 peso coin is at least 50% more than that of the 2 pesos coin.

It is a widespread practice to use the dominant peak of AdC namely (C-C/C-H) signal to calibrate the binding energy scales for the other XPS peaks. The (C-C/C-H) peak of AdC is set to be at a certain value in the range of 284.0–285.2 eV, and all other spectra are aligned accordingly [19]. This method was proposed by Siegbahn et al. [20] for the first time, and it was set to be at 285.0 eV by him, and it is still a common practice in many labs around the world to choose this reference point to calibrate the location of other core-level transition lines. However, by increasing the resolution of the commercial XPS system, it was revealed that C 1s binding energy, for example, could be related to the thickness of the hydrocarbon layer [21]. Therefore other reference points such as the Au 4f transition line [22,23] are suggested to be used to calibrate the binding energy.

In this study, the peak-fitting process of the AdC signal from the 1- and 2-pesos coins gave the value of 284.7 eV for the dominant peak (C-C/C-H) of the carbon, therefore we did not find any reason to calibrate the energy scale. In addition, the binding energy of $Cu^{(0)}$, $Ni^{(0)}$ peaks obtained from the coins coincide with those from the standard samples within the uncertainty of our measurements. The values of the other components of the AdC lines of the 1- and 2-pesos coins are listed in the Table 6 and are compared with the published values in reference [24]. In the case of the 1-peso coin, in addition to the other AdC lines component, we have detected an extra peak, which it is assigned to be related to metal-carbonate.

Fig. 7(A, B) shows the O 1s transition lines collected from the silvery part of the 1-peso of 1994 and that of the 2-pesos of 2016 coins, respectively. They are collected after sputtering the samples

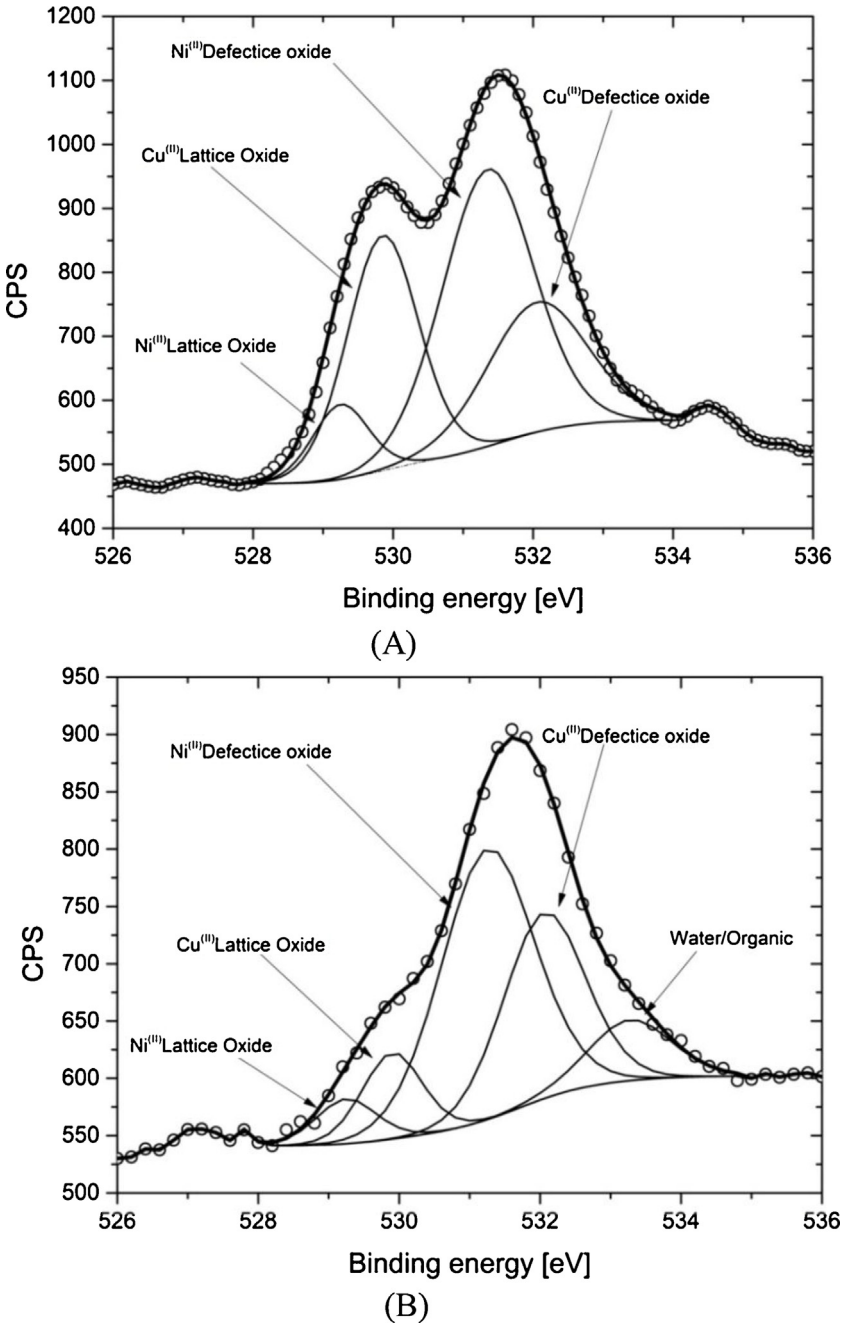

Fig. 7. O 1s spectra from silvery part of the 1-peso coin of 1994 (A) and the 2-pesso coin of 2016 (B).

Table 6
Adventitious carbon (AdC) line components of the 1- and 2-pesos coins in comparison to the published values in reference [24].

Component	1-peso [eV]	2-pesos [eV]	Reference [24] [eV]
C—C/C—H	284.7	284.7	284.8
C—O—C	286.1	286.2	~286.0
O—C=O	287.9	288.4	~288.5
Metal carbonate	290.1	--	288-290

with the 2 keV, Ar^+ ions for a period 1 min. For many transition metal oxides there are two main components that can be detected by XPS. The first one at lower binding energy is due to lattice oxide of the metals and the second one at higher binding energy is due to defective oxide of metals as suggested in reference [18]. This interpretation has also been confirmed by other experimental methods [25,26].

We were able to fit the spectra of O1s with the corresponding component of oxygen due to $Ni^{(II)}$ lattice oxide, at binding energy of 529.2 eV for the 1-peso and 529.3 e V for the 2-pesos coin. The peak at binding energy of 529.8 eV is ascribed as the contribution to $Cu^{(II)}$ lattice oxide for both the 1- and 2-pesos coins. In addition, the fitting process of the O 1s reveals an extra component for each coin owing to the contributions from the defective oxide of Ni, at the binding energy of 531.3 eV and 531.4 eV for the 1-peso and the 2-pesos coins, respectively. The contribution of Cu defective oxide was identified at the binding energy of 532.0 eV and 352.1 eV for the 1-peso and the 2-pesos coins, respectively. In the case of 1- peso coin, we have detected an extra peak at binding energy of 533.3 eV, which is assigned to be to the contribution of water/organic mate-

Table 7
O 1s peaks of the 1- and 2-pesos coins in comparison to the published values in references [16,17], the uncertainty in our measurement estimated to be 0.1 eV.

Component	1-peso [eV]	2-pesos [eV]	References [16],18] [eV]
$Ni^{(II)}$ Lattice oxide	529.2	529.3	529.30
$Cu^{(II)}$ Lattice oxide	529.8	529.8	529.68
$Ni^{(II)}$ Defective oxide	531.3	531.4	531.10
$Cu^{(II)}$ Defective oxide	532.0	532.1	531.99
Water/Organic	533.3	Not detected	532.80

Fig. 8. Photo of a 1-peso coin before and after exposure to the artificial sweat.

rial. The outcome of the peak fitting of O 1s XPS peak for 1- and 2 pesos coins are listed in Table 7. The values of the respective O 1s components obtained from references [16] and [18] are also listed.

Again comparison between the graphs in Fig. 7 indicates that the amount of metal oxide on the surface of the 1-peso coin is higher than that of the 2-pesos coin.

3.2. XPS spectra of the treated coins with the artificial sweat

Bimetallic corrosion is a well-known phenomenon, which take place when two metals or alloys with different potentials are in contact with an electrically conducting corrosive liquid, such as artificial sweat. A comprehensive study of the electrochemical behavior of the galvanic couple between the outer (ring) and the inner part of a 1-peso Argentine coins were performed and the results will be published in due course.

In the present work, only the results of corrosion tests performed under recommendations of ISO 3160-2 standard are presented. The test was performed by resting a cotton swab embedded in artificial sweat on a 1-peso coin for 24 hrs, see Fig. 8, and after that, the corroded region were analyzed by XPS in order to identify the nature of the corrosion products. The artificial sweat was prepared according to the ISO 3160 [27] standard: in one liter of distilled water we added 20 g/L sodium chloride, 17.5 g/L ammonium chloride, 5 g/L urea, 2.5 g/L acetic acid, and 15 g/L racemic lactic acid. The pH was then adjusted to 4.7 with 80 g/L NaOH solution. In all cases, the reagents used were analytical grade

Fig. 9 shows a typical Cu 2p spectrum from the corroded part of the 1-peso coin. Identification of the Ni or Al corrosion products was inconclusive, as it was expected, due to the detection limit of the XPS technique. The atomic concentration of Ni and Al in the golden part of coin are nominally %2 and %6, respectively. In addition, identification of aluminum and aluminum oxide chemical states in a

Table 8
Binding energies of the Cu 2p XPS peak and its satellite peaks from the corroded region after 4 cycles of Ar^+ cleaning and those from reference [16].

	Main peak [eV]			Satellite peaks [eV]		
Binding energy	932.3	934.8	937.9	942.6	944.5	946.5
[(a)] Binding Energy	N/A	934.67	N/A	939.30	942.20	944.12

[(a)] From reference [16].

sample containing copper comes with a large uncertainty due to the interferences of Cu 3s and Cu 3p XPS peaks with the Al 2s and Al 2p peaks.

All the components in the spectrum are fitted with GL(30) line shapes, and a modified U2 Tougaard background type, as defined in the CasaXPS software, was applied to remove the contribution of the inelastic electron scattering. A simple Shirley background will cut through the spectra, and a simple Tougaard background results in a background relatively far from the raw data. The Cu 2p binding energy region comprises of two main components, $2p_{3/2}$ and $2p_{1/2}$, due to the spin-orbit splitting. These two components are well separated (around 20 eV), therefore only the Cu $2p_{3/2}$ peak has been analyzed to identify the various copper chemical states.

The binding energies, derived from the curve fitting of $Cu2p_{3/2}$ region are listed in Table 8. Three major components are fitted for the main peak of Cu $2p_{3/2}$: One component at binding energy of (932.3 ± 0.1) eV, which is assigned to $Cu^{(I)}$, it can be attributed to species such as cuprous chloride (CuCl), cuprous oxide (Cu_2O), and the reduction of $Cu^{(II)}$ products to $Cu^{(I)}$ under XPS analysis and Ar^+ ions cleaning process. The reduction of $Cu^{(II)}$ to $Cu^{(I)}$ is well known and has been reported previously [28,29,30]. We have verified this fact by collecting the spectra repeatedly after (8 cycles) of 2 min 2 keV Ar^+. The comparison of spectra, (not reported here) reveals an increase of the $Cu^{(I)}$ component at the expense of $Cu^{(II)}$ component.

The second component is located at binding energy of (934.8 ± 0.1) eV, which is assigned to $Cu^{(II)}$ species. It can be in the form of cupric hydroxide $Cu(OH)_2$, and cupric carbonate ($CuCO_3$). The $Cu^{(II)}$ carbonate is a likely substance, since the $Cu^{(II)}$ hydroxide is rarely found as an uncombined substance because it reacts with carbon dioxide in the air and form a basic copper$^{(II)}$ carbonate, through a chemical reaction as given below:

$$2Cu + H_2O + CO_2 + O_2 \rightarrow Cu(OH)_2 + CuCO_3$$

As a matter of fact, the green-bluish patina which forms on the copper alloy statues in the cities is in principle a 1:1 mol mixture of $Cu(OH)_2$ and $CuCO_3$ [31]. Finally, a third peak was fitted at higher binding energy of (937.9 ± 0.1), which we assigned to $Cu^{(II)}$ chloride di-hydrate; $CuCl_2(H_2O)_2$. We imply that $Cu^{(II)}$ chloride $CuCl_2$, which is a light brown solid, forms during the exposure of the coin with the artificial sweat. It will then absorb water molecules to form a blue-green di-hydrate.

In addition to the main peak, a structure seen at higher binding energy in the range of 942-947 eV which were fitted with three satellite peaks at the binding energies of (942.6 ± 0.2) eV, (944.5 ± 0.2) eV, and (946.5 ± 0.2) eV.

Appearance of satellite peaks due to $Cu^{(II)}$ above the main peaks of Cu $2p_{3/2}$ and Cu $2p_{1/2}$, in the range of 939–945 eV and 959–964 eV is a well-known phenomena [14,15,16].

The existence of these satellite lines are understood as a consequence of a simple charge-transfer model explained in [32,33]. They suggest the main peaks are corresponding to $(2p^5 3d^{10} C)$ final states, whereas the satellite structures correspond to $(2p^5 3d^9)$ final states (here C core hole after the process of charge-transfer).

In the literature, a range of different shapes of satellite peaks are reported for $Cu^{(II)}$ in general and $Cu(OH)_2$ in particular, see for instance references [34,35]. The number of peaks, which has been used to fit the satellite structure are also different, it varies between

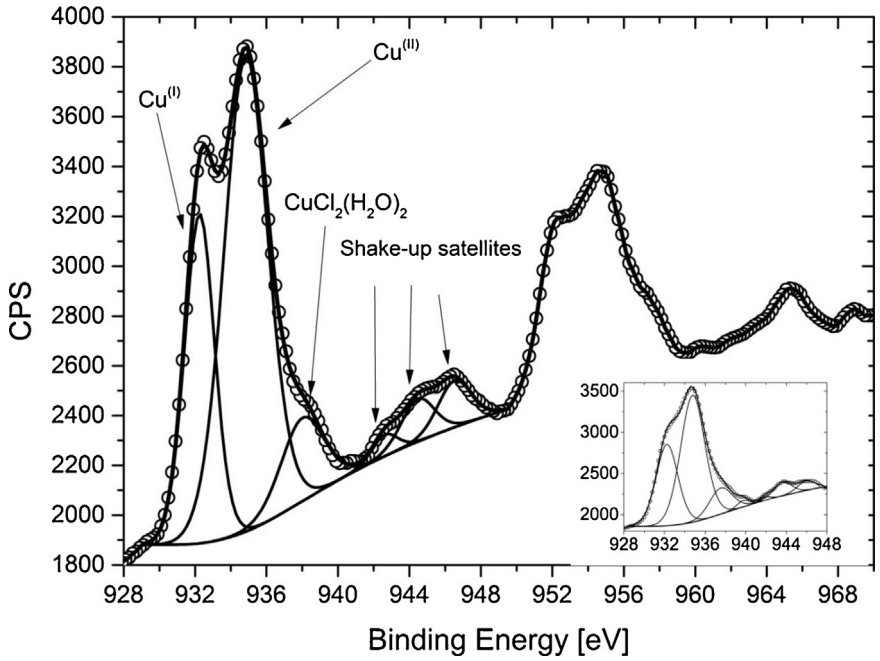

Fig. 9. Cu 2p XPS peak obtained from the corrosion product after four cycles of Ar^+ ions treatments, inset is the Cu $2p_{3/2}$ XPS peak after three cycles of Ar^+ ions cleaning.

1 to 3 [14,17,36]. These discrepancies could be due to the resolution of the XPS system. For instance, M. C. Biesinger et al. [16] reported 1 peak for the main transition line, and 3 peaks for the satellite structure for a pure $Cu(OH)_2$ standard sample, which are listed below in Table 8 along with our results. The authors report a peak at the binding energy of 934.67 eV for the main transition line.

In addition to the peaks at the binding energies of 942.20 eV and 944.12 eV, they were also able to fit an extra peak at binding energy of 939.30 eV for the satellite formation. The positions of our first- and second-satellite peaks are comparable with the positions of their second- and third-satellite peaks.

In some of our energy scans from the corroded region, we needed also an extra satellite peak, similar to reference [16], in the range of (939.0-940.0) eV, to be able to fit the satellite structure. We discovered a direct relationship between the ratio of the $Cu^{(I)}$ and $Cu^{(II)}$, (which is changing due to the effect of Ar^+ bombardment) and the appearance of this peak in particular and the shape of the satellite structure in general, (see inset in Fig. 9). The main spectrum in the Fig. 9 shows the Cu 2p collected after four cycles of Ar^+ cleaning, whereas the inset shows the Cu $2p_{3/2}$ XPS peak after three cycles of Ar^+ ions cleaning. Not only we have observed an increase in the intensity of $Cu^{(I)}$ peak after four cycles of Ar^+ cleaning in comparison to that after three cycles of Ar^+ ions cleaning, but also the shape of the satellite structure has been changed. It is an interesting fact and further investigations are needed to verify this, which is beyond the scope of the current paper.

In order to support our findings and the identifications of the copper chemical states, XPS spectra were also collected from the Cl 2p, and O 1s binding energy regions. Fig. 10 shows the XPS spectrum of Cl 2p binding energy. The spectrum was fitted with two pairs of constrained doublets. The separation of the major peak from the minor peak in each doublet was set to be 1.6 eV and the area of the minor peak was constrained to half of that of the major peak, as it is expected from Cl $2p_{3/2}$ and Cl $2p_{1/2}$ peaks. The fitting process resulted in an envelope which matches remarkably with the raw data. The binding energies of the components of each doublet are listed in the Table 9. Similar values are reported in [37] and [10], and references therein.

Table 9
The Cl 2p XPS peak obtained from the corrosion product.

	CuCl-doublet [eV]		$CuCl_2$-doublet [eV]	
Binding Energy	198.4	200.1	201.0	202.6

Fig. 11 presents the O 1s XPS spectra acquired from the corrosion product after 4 cycles of Ar^+ ions cleaning. It has different characteristics in comparison to the O 1s peaks in Fig. 7 of the untreated coin with artificial sweat. The analysis of the O 1s peak verifies our interpretation of the Cu 2p XPS peak and confirms our identifications of the Cu chemical states.

The O 1s spectrum was fitted with three components. The GL(30) line shape and a Shirley back ground was used to remove the contribution of the inelastic electron scattering. The main peak in the O 1s region centered at the binding energy of (533.5 ± 01) eV is ascribed to the contribution of the copper carbonate and the second larger component located at the binding energy of (531.3 ± 0.1) eV is attributed to the copper hydroxide, and finally the component at the binding energy of (529.2 ± 0.1) eV can be due to the possible small amount of metal oxide at the surface.

4. Discussion

The concept of segregation of the binary metal alloys in general [38,39] and Cu-Ni alloy in particular [40,41] is well-known and has been studied heavily. The major part of the earlier investigations is pointing in the direction of the Cu surface enrichment rather than Ni surface enrichment, independent of the ratio of Cu/Ni bulk concentration. However, in a more recent study [42], the experimental results of solute Ni segregation to the surface in $Ni_{1-x}Cu_x$ alloys, (X is in the range of 0.8-1.0) has been reported, in contrast to the earlier believe that the Cu atoms always segregate to the surface. The authors made also an interesting observation in connection to another investigation on the catalytic activity of Ni-Cu alloys in cyclohexane dehydrogenation into benzene [43].

In reference [43], the authors reported their measurements of the chemical reaction as a function of Cu-Ni alloy composition. They observed a rapid increase as Cu bulk concentration increases from

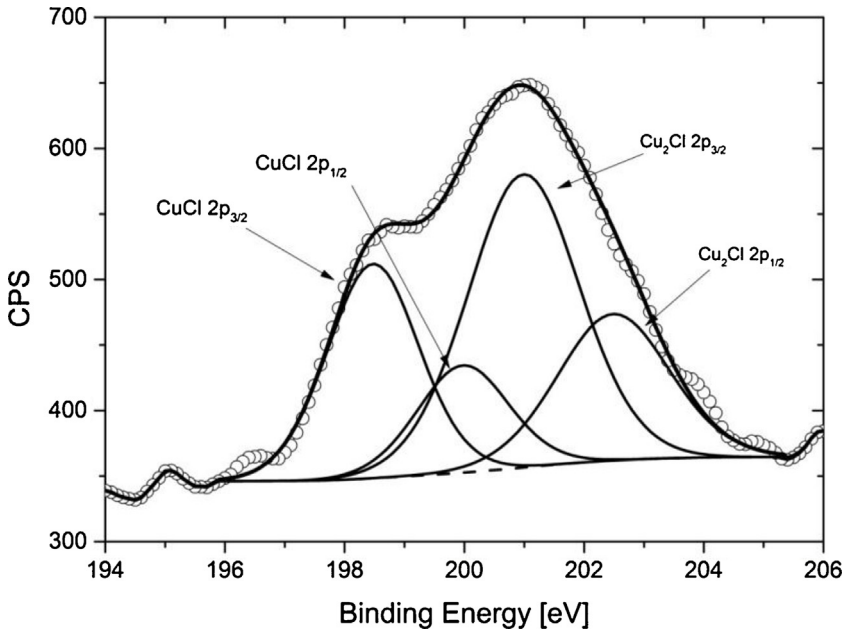

Fig. 10. Cl 2p XPS peak obtained from the corrosion product.

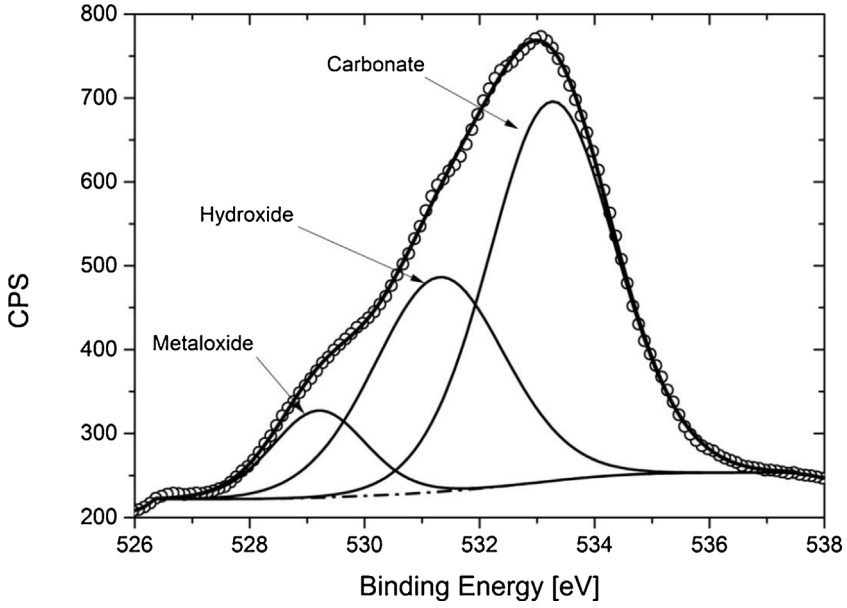

Fig. 11. O 1s XPS peak obtained from the corrosion product.

0 to 5%, it reaches a plateau in the Cu concentration in the range of (10-80)%, and again decreases as the Cu bulk concentration further increases to 100%. They interpreted the initial rapid increase in the catalytic activity is due to Cu enrichment at the surface, but they were not been able to explain the steep drop in the Ni solute range. Other evidence of the Ni segregation is presented in [44], the authors investigated the surface segregation of $Ni_{1-x}Cu_x$ alloy (where X = 3, 6, 9, 15, 20, 30, 45, 80, 90, and 95) using a Time of Flight (ToF) atom probe. They observed that solute elements tend to segregate to surface upon annealing in the temperature of 300 °C to 600 °C, namely the Ni atoms segregate in the Cu rich alloys, whereas the Cu atoms segregate in the Ni rich alloys.

It is of interest to point out that all the investigations on the surface segregation of the Cu-Ni alloys, mentioned above, were carried out at higher temperatures than the room temperature. However, the higher temperature will only increase the activation energy and reduce the time of the segregation process. It means that the surface segregation can also happen at room temperature but during longer period of time. We consider that Ni segregation actually take place for the coins made of the Cu-Ni alloy, where the bulk concentration of the Cu is higher than that of the Ni, such as the coins in the current study, and the euro coins. In contrast to the interpretation of the earlier study [9], we believe that the surface segregation of Ni of the Cu-Ni coins is actually, an intrinsic phenomenon, where external factors during the circulation time of the coins can accelerate the process.

To understand the reason for the discrepancy in the ratio of atomic concentration of Cu/Ni between the particular coins used in the current study, one has to bear in mind that what is detected on the surface of the coins is a product of the interplay of 2 dynamic processes that happen simultaneously to the coins during the

circulation time, namely surface segregation of the constituent atoms and removal of Ni from the surface.

There are countless of references that confirm Ni can be removed from the surface of coins by rubbing and handling with hands and physical contact with any other objects such as a wallet or even bank paper notes. We have cited a few of them (references 1-5) in the Introduction section. In a recent study [45], the author designed and developed an experimental strategy for assessment of short and frequent skin exposure to nickel containing consumer products in daily life. The author, in this study, reports the presence of nickel on the skin after only a single contact with all the Ni-containing objects. Therefore, the process of Ni-release from the surface of the Ni-containing alloy of daily usage objects such as coins is well established. It was also demonstrated that the Ni can be removed easily from the surface by handling with hands.

The other process which defines the chemical composition of the coin surface is the surface segregation in the bimetallic alloys, which depends on a few major factors, such as the atomic radii of the metals, their surface free energy, and the oxide formation enthalpy of the metals.

The atomic radii of Cu and Ni are very similar (128 pm and 124 pm), respectively [46]. Therefore, size difference does not play an important role with respect to the surface segregation in this system. One can draw a ‘parallelism’ between the ‘atomic size effect’ in the bimetallic alloys and the so called ‘brazil nut effect’, where in a container of mixed nuts with different sizes, the bigger nuts tend to raise on the surface. In a Cu-Ni alloy system ‘the nuts’ have almost the same size.

The process of surface segregation was theoretical studied by Gibbs [47]. The significant result of this study is the so called Gibbs adsorption isotherm equation given by:

$$\Gamma_A = -\left(\frac{\partial\sigma}{\partial\mu_A}\right)_{T,P}$$

where Γ_A is termed the ‘surface surplus’ of component A (in an arbitrary A-B binary system), σ is the surface free energy or sometimes called surface tension for liquids, and μ_A is the chemical potential of A. In plain English, what the above-mentioned equation implies, is that a constituent element which can lower the surface free energy will be segregated to the surface and the concentration of that atom increases at the surface region.

Consequently, according to the Gibbs adsorption isotherm equation, Cu is expected to segregate towards the surface due to its lower surface free energy [48]. This would be true if the alloy was in the vacuum, in the absence of surface adsorbates. The condition is more complex for the Cu-Ni alloy in the air, due to chemisorptions induced surface segregation. The presence of oxide and oxygen-containing adsorbates such as H_2O, CO_2, CO, and predominantly oxygen itself in the air will change the circumstances [49].

For the bimetallic system of Cu-Ni in air, the Gibbs free energies for NiO, Cu_2O and CuO are −211.7104 kJ/mol, −146.0216 kJ/mol, −157.3184 kJ/mol [50]. The Gibbs free energy for NiO is lower than that of both Cu_2O and CuO. This means that in the Cu-Ni alloys, the Ni preferentially segregating to the surface and Cu inwards. For a surface of any bulk bimetallic alloy, the large volume inside can act only as a semi-infinite source for one atom and a sink for the other [51].

The role of the oxygen chemisorptions induced segregation is probably more important than all other gases, in which the oxygen of the air preferentially pulls one component to the surface and thus enriches the surface in that component. The enthalpy values for the formation of NiO (-239.7432 kJ/mol), Cu_2O (-168.6152 kJ/mol) and CuO (-129.704 kJ/mol) (49) indicate that Ni oxide is formed more easily than Cu oxides. In other words, the oxygen literally ‘drags’ the Ni atoms to the surface. Based on the thermodynamically argument given above one can only expect that Ni to be concentrated on the surface of the coins.

A vast different theoretical approach and models are proposed to describe the surface segregation phenomena in bimetallic alloys [52], and the references therein. However, they all have one principle in common: that the surface segregation occurs in the 5-10 nm outermost layer (selvedge) of the alloy. It is important to emphasize that the surface enrichment phenomenon is not the same as the diffusion of the atoms from the bulk to the surface due to the heat and/or concentration gradient.

In our upcoming paper, we have reported that 1-peso Argentine coins were immersed in the artificial sweat solution during 1 week and, after that, a chemical analysis of the solution were performed with the Inductively Coupled Plasma Optical Emission Spectrometry (ICP-OES) technique. We have measured the concentration of Ni dissolved in the artificial sweat on average to be 2.9 ± 0.1 ppm [53]. This means that Ni atoms not only have been segregated to the surface but also have been released from the coins during only one week of exposure to the artificial sweat. For the bimetallic alloy in an aqueous environment, other factor operates that accelerate the surface segregation of the constituent atoms, namely water-induced surface segregation [54]. Our preliminarily XPS studies on these coins confirm also the depletion of Ni at the surface, similar to the results we obtained from the coin minted in 2016.

In the light of the above argument, we believe that it is established that thermodynamically Cu-enrichment on the surface is not plausible for the coins under investigation in the current study. The Ni-depletion on the surface of the coin from 2016 can only be explained that the Ni atoms after the process of the surface segregation have been removed by physical contacts with hands or other objects. On the other hand, the observed Ni-enrichment on the coin from 1994 can only be explained that either it did not go through the same removal process by the external objects as for the coin from 2016, or the contamination on the surface which is considerably more than that for the coin from 2016, prevented the Ni atoms to be removed from the surface.

Finally, it is of interest to mention that the other feature, the depth profiling of the coin from 2016 reveals, is that the diffusion of Ni atoms from the bulk to surface did not take place during the circulation time, despite a clear existence of concentration gradient between the bulk and the surface. This can be explained as the diffusion of Ni from the bulk to the surface needs more energy than the process of the surface segregation. Therefore, for the alloys at low temperature ambient, the diffusion process, if it is possible at all, would take infinite time to occur.

5. Conclusion

The surface of the ring and centre part of 1-peso of 1994 and 2-pesos of 2016 Argentine have been studied by means of the XPS. It has been observed that nickel and copper on the surface of the untreated coins present in the form of $Cu^{(0)}$, $Cu^{(II)}$, and $Ni^{(0)}$, $Ni^{(II)}$, respectively. Examination of the O 1s peak position and its component confirm our identifications of the chemical states of the metals. In addition, the fitting process of the Ni 2p XPS spectrum also shows a multiplet splitting for $Ni^{(0)}$ and $Ni^{(II)}$. The position of Shake-up lines also confirms the existence of the nickel oxide in the form of $Ni^{(II)}$. Depth profiles were acquired from the silvery part of the coins, and the ratio of the metallic concentration were determined within the 15 nm depth. We observed nickel enrichment at the expense of copper on the surface of the silvery part of the 1-peso coin of 1994, whereas the result from 2-pesos of 2016 coin shows the reverse, namely lack of Ni in comparison to Cu within 15 nm depth. By comparison of the Cu 1s and O 1s XPS spectra obtained from the coins, we proposed an explanation to this discrepancy. The

depth profiling from the golden part of the coins is inconclusive due to the small amount of the Ni (nominally %2).

Additionally, oxidation of the golden part of the coins with the artificial sweat in air for 24 hrs reveals mainly the formation of copper hydroxide, and copper carbonate on the surface. By examining the Cl 2p XPS peak, we can also conclude the formation of the $Cu^{(I)}$- and $Cu^{(II)}$- chloride on the surface.

Acknowledgments

F. S. Gard would like to acknowledge Professor Enrique Garcia Michel for a constructive and fruitful discussion about the methodology used in the current work and for proof reading the revised version of the manuscript.

References

[1] J.P. Thyssen, A. Linneberg, T. Menné, J.D. Johansen, The epidemiology of contact allergy in the general population - prevalence and main findings, Contact Dermat. 57 (2007) 287–299.
[2] C.D. Calnan, Nickel dermatitis, Br. J. Dermatol. 68 (1956) 229–236.
[3] S.E. Jacob, J.N. Moenrich, B.A. Mckean, M.J. Zirwas, J.S. Taylor, Nickel allergy in the United States: A public health issue in need of a "nickel directive, J. Am. Acad. Dermatol. 60 (2009) 1067–1069.
[4] N.B. Pedersen, S. Fregert, P. Brodelius, B. Gruvberger, Release of nickel from silver coins, Acta Dermatovener 54 (1974) 231–234.
[5] F.O. Nestle, H. Speidel, M.O. Speidel, High nickel release from 1- and 2-euro coins, Nature 419 (2002) 132.
[6] European Parliament and Council directive 94/27/EEC Official Journal of the European Communities (Brussels, 1994).
[7] Council regulation (SC) 975/98 of 3rd May 1998 on denominations and technical specifications of euro coins intended for circulation. Official Journal L139, 11 May (1998) 6-8.
[8] J.P. Thyssen, D.J. Gawkroger, I.R. White, A. Julander, T. Menné, C. Lidén, Coin exposure may cause allergic nickel dermatitis; a review, Contact Dermat. 68 (2012) 3–14.
[9] F. Gou, M.A. Gleeson, J. Villette, S.E.F. Kleyn, A.W. Kleyn, The surface of 1-euro oins studied by X-ray photoelectron dermatitis; a review, Contact Dermat. 68 (2012) 3–14.
[10] C. D. Wagner, A.V. Naumkin, A. Kraut-vass, J.W. Allison, C.J. Powell, J.R. Rumble Jr., NIST Standard Reference Database 20, Version 3.4 (web version), http://srdata.nist.gov/xps/.
[11] A.P. Grosvenor, M.C. Biesinger, R.St.C. Smart, N.S. McIntyre, New interpretations of XPS of nickel and oxides, Surf. Sci. 600 (2006) 1771–1779.
[12] S. Hufner, Photoelectron spectroscopy Solid State Science Series, vol. 82, Springer-Verlag, 1995 (Chapter3).
[13] N. Pauly, S. Tougaard, F. Yubero, Determination of the Cu 2p primary excitation spectra for Cu, Cu_2O and CuO, Surf. Sci. 620 (2014) 17–22.
[14] D.A. Zatsepin, V.R. Galakhov, M.A. Korotin, V.V. Fedorenko, E.Z. Kurmaev, S. Bartkowski, M. Neumann, R. Berger, Valence states of copper ions and electronic structure of $LiCu_2O_2$, Phys. Rev. B. 57 (8) (1998) 4377–4381.
[15] S. Colin, E. Beche, R. Berjoan, H. Jolibois, An XPS and AES study of the free corrosion of Cu-, Ni- and Zn-based alloys in synthetic sweat, Corros. Sci. 41 (1999) 1051–1065.
[16] M.C. Biesinger, L.W.M. Lau, A.R. Gerson, Rst.C. Smart, Resolving surface chemical states in XPS analysis of first row transition metals, oxides and hydroxides: Sc, Ti, V, Cu and Zn, Appl. Surf. Sci. 257 (2010) 887–898.
[17] Y.S. Chen, J.F. Kang, B. Chen, B. Gao, L.F. Liu, X.Y. Liu, Y.Y. Wang, L. Wu, H.Y. Yu, J.Y. Wang, Q. Chen, E.G. Wang, Microscopic mechanism for unipolar resistive switching behavior of nickel oxides, J. Phys. D: Appl. Phys. 45 (2012) 1–6, 065303.
[18] M.C. Biesinger, B.P. Payne, L.W.M. Lau, A. Gerson, R.St.C. Smart, X-ray photoelectron spectroscopic chemical state quantification of mixed nickel metal, oxide and hydroxide systems, Surf. Interface Anal. 41 (2009) 324–332.
[19] P. Swift, Adventitious carbon - the panacea for energy referencing, Surf. Interface Anal. 4 (1982) 47–51.
[20] K. Siegbahn, C. Nordling, A. Fahlman, R. Nordberg, K. Hamrin, J. Hedman, G. Johansson, T. Bergmark, S.-E. Karlsson, I. Lindgren, B. Lindberg, ESCA—Atomic, Molecule and Solid State Structure Studied by Means of Electron Spectroscopy, Almqvist & Wiksells Boktryckeri, Uppsala, 1967.
[21] S. Kohiki, K. Oki, Problems of adventitious carbon as an energy reference, J. Electron. Spectrosc. Relat. Phenom. 33 (1984) 375–380.
[22] Th. Gross, M. Ramm, H. Sonntag, W. Unger, H.M. Weijers, E.H. Adem, 59, Surf. Interface Anal. 18 (1992).
[23] A.C. Miller, C.J. Powell, U. Gelius, C.R. Anderson, Energy calibration of X-ray photoelectron spectrometers. part III: location of the zero point on the binding-energy scale, Surf. Interface Anal. 26 (1998) 606–614.
[24] http://xpssimplified.com/elements/carbon.php.
[25] H.A.E. Hagelin-Weaver, J.F. Weaver, G.B. Hoflund, G.N. Salaita, Electron energy loss spectroscopic investigation of Ni metal and NiO before and after surface reduction by Ar++ bombardment, J. Electron. Spec. Rel. Phenom. 134 (2004) 139–171.
[26] P.R. Norton, G.L. Tapping, J.W. Goodale, A photoemission study of the interaction of Ni(100), (110) and (111) surfaces with oxygen, Surf. Sci. 65 (1) (1977) 13–36.
[27] ISO 3160-2: Watch-Cases and Accessories - Gold Alloy Coverings - Part 2: Determination of Fineness, Thickness, Corrosion Resistance and Adhesion, 2003.
[28] Wu Chun-Kwei, M. Yin, S. O'Brien, J.T. Koberstein, Quantitative analysis of copper oxide nanoparticle composition and structure by X-ray photoelectron spectroscopy, Chem. Mater. 18 (25) (2006) 6054–6058.
[29] Y. Iijima, N. Niimura, K. Hiraoka, Prevention of the reduction of CuO during X-ray photoelectron spectroscopy analysis, Surf. Interface. Anal. 24 (3) (1996) 193–197.
[30] D.F. Mitchell, G.I. Sproule, M.J. Graham, Sputter reduction of oxides by ion bombardment during Auger depth profile analysis, Surf. Interface Anal. 15 (8) (1990) 487–497.
[31] A.M. Salvi, F. Langerame, A. Macchia, M.P. Sammartino, M. Laurenzi Tabasso, XPS characterization of (copper-based) colored stains formed on limestone surfaces of outdoor Roman monuments, Chemistry Central J. 6 (Suppl. 2) (2012) 1–13, S10.
[32] G. Van der Laan, C. Westra, C. Haas, G.A. Sawatzky, Phys. Rev. B 23 (1981) 4369–4371.
[33] J. Zaanen, C. Westra, G.A. Sawatzky, Phys. Rev. B 33 (1986) 8060–8066.
[34] http://www.xpsfitting.com/2012/08/shake-up-structure.html.
[35] O. Akhavan, R. Azimirad, S. Safad, E. Hasanie, $CuO/Cu(OH)_2$ hierarchical nanostructures as bactericidal photocatalysts, J. Mater. Chem. 21 (2011) 9634–9640.
[36] E. Cano, C.L. Torres, J.M. Bastidas, An XPS study of copper corrosion originated by formic acid vapour at 40% and 80% relative humidity, Materials and corrosion 52 (2001) 667–676.
[37] Sh. Elzey, J. Baltrusaitis, Sh. Bianb, V.H. Grassian, Formation of paratacamite nanomaterials via the conversion of aged and oxidized copper nanoparticles in hydrochloric acidic media, J. Mater. Chem 21 (2011) 3162–3169.
[38] R.N. Barnett, U. Landman, C.L. Cleveland, Surface segregation in simple metal alloys: an electric theory, Phys. Rev. B 28 (1983) 6647–6658.
[39] J.J. Burton, E. Hyman, D.G. Fedak, Surface segregation in alloys, J. Catal. (1975) 106–113.
[40] H.H. Brongersma, T.M. Buck, Selected topics in low-energy ion scattering: surface segregation in cu/ni alloys and ion neutralization, Surf. Sci. 53 (1975) 649–658.
[41] Masao Kuniaki Watanabe, Hashiba, Toshiro Yamashina, A quantitative analysis of surface segregation and in-depth profile of copper-nickel alloys, Surf. Sci. 61 (1976) 483–490.
[42] T. Sakurai, T. Hashizume, A. Jimbo, A. Sakai, S. Hyodo, New result in surface segregation of Ni-Cu binary alloys, Phys. Rev. Lett. 55 (5) (1985) 514–517.
[43] J.H. Sinfelt, Bimetallic Catalysts: Discoveries, Concepts, and Applications, Wiley, New York, 1983.
[44] T. Hashizume, A. Jimbo, T. Sakurai, Surface segregation of Cu-Ni alloys, Journal de Physique (1984), Colloque C9, supplément No. 12, Tome 45.
[45] B. Erfani, Thesis for Master's Degree in Toxicology, Strategy to Assess Short and Frequent Skin Contacts With Nickel, Karolinska institutet, Sweden, 2013.
[46] L. Pauling, Atomic radii and interatomic distances in metals, J. Am. Chem. Soc. 69 (1947) 542–553.
[47] J.W. Gibbs, Collected Works, vol, I, Yale University Press, New Haven, Connecticut, 1948, pp. 219–233.
[48] A.V. Ruban, H.L. Skriver, J.K. Nørskov, Surface segregation energies in transition-metal alloys, Phys. Rev. B 59 (1999) 15990–16000.
[49] D. Tomanek, S. mukhjerjee, V. kumar, K.H. Bennemann, Calculation of chemisorption and absorption induced surface segregation, Surf. Sci. 114 (1982) 11–22.
[50] http://www.drjez.com/uco/ChemTools/Standard%20Thermodynamic%20Values.pdf.
[51] L. Peng, E. Ringe, R.P. Van Duyne, L.D. Marks, Segregation in bimetallic nanoparticles, Phys. Chem. Chem. Phys. (2015), http://dx.doi.org/10.1039/c5cp01492a.
[52] J.K. Strohl, Modeling Alloy Catalyst Surface and Bimetallic Catalyst Particles, PhD Thesis, Iowa State University, USA, 1988.
[53] G. Duffo, S. Farina y S. Fernandez, F. S. Gard, Electrochemical studies of the galvanic corrosion of $1 Argentine coins, to be published.
[54] B. Zhu, Y Gao, Water-induced bimetallic alloy surface segregation: A first principle study, arXiv:1601.02346v1 (cond-mat.mtrl-sci).